CTD Tyrosine Phosphorylation Impairs Termination Factor Recruitment to RNA Polymerase II

Andreas Mayer *et al.*

Science **336**, 1723 (2012);
DOI: 10.1126/science.1219651

28. A. L. Németh *et al.*, *FEBS J.* **274**, 1610 (2007).
29. N. Netzer *et al.*, *Nature* **462**, 522 (2009).
30. R. J. Jackson, S. Napthine, I. Brierley, *RNA* **7**, 765 (2001).
31. M. Sisido, in *Chemical Biology: From Small Molecules to Systems Biology and Drug Design*, S. L. Schreiber, T. M. Kapoor, G. Wess, Eds. (Wiley-VCH Verlag, Weinheim, Germany, 2007), vol. 1, pp. 271–284.
32. R. Geslain, T. Pan, *J. Mol. Biol.* **396**, 821 (2010).
33. S. E. Dmitriev *et al.*, *J. Biol. Chem.* **285**, 26779 (2010).
34. M. A. Skabkin *et al.*, *Genes Dev.* **24**, 1787 (2010).
35. W. C. Merrick, W. F. Anderson, *J. Biol. Chem.* **250**, 1197 (1975).
36. S. L. Adams, B. Safer, W. F. Anderson, W. C. Merrick, *J. Biol. Chem.* **250**, 9083 (1975).
37. J. H. Kim, S. M. Park, J. H. Park, S. J. Keum, S. K. Jang, *EMBO J.* **30**, 2454 (2011).
38. Materials and methods are available as supplementary materials on *Science* Online.

Acknowledgments: We thank K. Collins, A. H. Bakker, K. Chen, N. Nagarajan, and T. Greene for helpful discussions and advice; Y. Ow for initial experiments with NSC119893; and N. Nagarajan and K. Lind for assistance with intravenous injections. The data presented in this paper are tabulated in the main paper and in the supplementary materials. S.R.S. was supported in part by an NIH training grant, a postdoctoral fellowship from the Cancer Research Institute, and a National Research Service Award (NRSA) fellowship from the NIH. M.P.-E was supported by an NIH training grant and by the Ruth Kirschstein NRSA predoctoral fellowship. This research was supported by grants from the NIH to N.S. and T.P. and the International AIDS Vaccine Initiative to N.S. The authors declare no competing financial interests.

Supplementary Materials

www.sciencemag.org/cgi/content/full/336/6089/1719/DC1
Materials and Methods
Figs. S1 to S10
Table S1
References (*39*–*42*)

8 February 2012; accepted 25 April 2012
10.1126/science.1220270

CTD Tyrosine Phosphorylation Impairs Termination Factor Recruitment to RNA Polymerase II

Andreas Mayer,[1]* Martin Heidemann,[2]* Michael Lidschreiber,[1] Amelie Schreieck,[1] Mai Sun,[1] Corinna Hintermair,[2] Elisabeth Kremmer,[3] Dirk Eick,[2]† Patrick Cramer[1]†

In different phases of the transcription cycle, RNA polymerase (Pol) II recruits various factors via its C-terminal domain (CTD), which consists of conserved heptapeptide repeats with the sequence Tyr[1]-Ser[2]-Pro[3]-Thr[4]-Ser[5]-Pro[6]-Ser[7]. We show that the CTD of transcribing yeast Pol II is phosphorylated at Tyr[1], in addition to Ser[2], Thr[4], Ser[5], and Ser[7]. Tyr[1] phosphorylation stimulates binding of elongation factor Spt6 and impairs recruitment of termination factors Nrd1, Pcf11, and Rtt103. Tyr[1] phosphorylation levels rise downstream of the transcription start site and decrease before the polyadenylation site, largely excluding termination factors from gene bodies. These results show that CTD modifications trigger and block factor recruitment and lead to an extended CTD code that explains transcription cycle coordination on the basis of differential phosphorylation of Tyr[1], Ser[2], and Ser[5].

The C-terminal domain (CTD) is a flexible, tail-like extension of RNA polymerase (Pol) II and consists of 26 (yeast) or 52 (human) highly conserved heptapeptide repeats of the consensus sequence Tyr[1]-Ser[2]-Pro[3]-Thr[4]-Ser[5]-Pro[6]-Ser[7]. During the transcription cycle, changes in CTD phosphorylation patterns coordinate the recruitment of transcription and mRNA processing factors to Pol II (*1*–*3*). During early transcription, Ser[5] phosphorylation recruits the mRNA capping enzyme (*4*, *5*). Ser[2] phosphorylation occurs during transcription elongation and functions in recruitment of RNA 3′-processing and termination factors (*6*). Phosphorylations at Ser[7] (*7*–*9*) and Thr[4] (*10*) have roles in processing of specific RNAs. Tyr[1] phosphorylation was described for human Pol II almost two decades ago (*11*), but whether this has a functional role and whether it exists in other species are unknown.

We generated a monoclonal antibody against a Tyr[1]-phosphorylated CTD peptide (3D12, Methods). Because the functional CTD unit is a pair of repeats (*12*), we determined antibody specificity by using di-heptapeptides bearing combinations of phosphorylations (Fig. 1A and fig. S1). This revealed a high affinity for the Tyr[1]-phosphorylated CTD that was not impaired by adjacent Ser[2] phosphorylation and no affinity to other CTD peptides (Fig. 1A and fig. S1). The antibody immunoprecipitated Pol II from extracts of the yeast *Saccharomyces cerevisiae* (Fig. 1B), and the precipitated polymerases were also phosphorylated at Ser[2], Ser[5], and Ser[7] (fig. S2). The antibody also recognized Pol II that was purified from human cells with antibody 1C7 (fig. S1) and phosphorylated in vitro by the Tyr[1] kinase c-Abl (*13*) (Fig. 1C). Thus, antibody 3D12 specifically recognizes the Tyr[1]-phosphorylated CTD, and Tyr[1] phosphorylation occurs in yeast.

To investigate whether genome-associated Pol II is phosphorylated at Tyr[1], we used high-resolution chromatin immunoprecipitation (ChIP) profiling in proliferating yeast (*14*). Data from two biological replicates (R = 0.94) were averaged and revealed strong signals over protein-coding and small nucleolar RNA genes (fig. S3). To test whether Tyr[1] phosphorylation occurs on all transcribed protein-coding genes, we measured covariation in ChIP data for other CTD phosphorylations by singular value decomposition (*14*). The first singular vector explained 83.8% of the variance (fig. S4), indicating a similar occurrence of phosphorylations at Tyr[1],

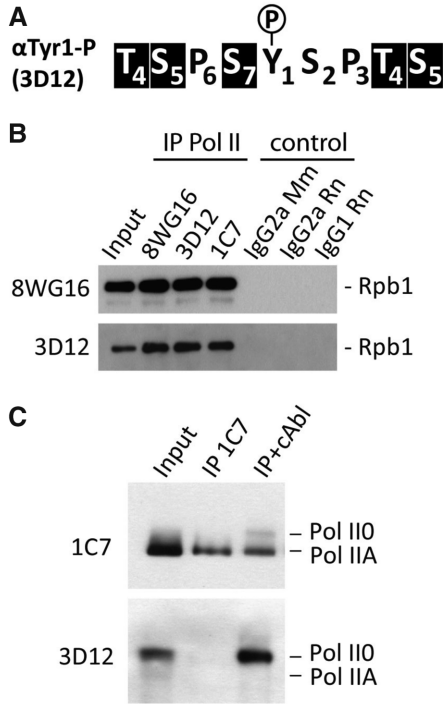

Fig. 1. Pol II CTD is phosphorylated at Tyr[1]. (**A**) Part of the CTD sequence around phosphorylated Tyr[1] (Y_1). Residues Ser[2], Pro[3], Thr[4], Ser[5], Pro[6], and Ser[7] are denoted S_2, P_3, T_4, S_5, P_6, and S_7, respectively. CTD residues that interfere with 3D12 antibody binding upon phosphorylation are highlighted in black. (**B**) Western blot analysis of whole-cell extract from proliferating yeast (Input). Pol II was immunoprecipitated with antibodies 8WG16, 3D12, and 1C7 (IP Pol II) and probed with 8WG16 or 3D12. Isotype controls are shown. Ig, immunoglobulin. (**C**) Antibody 3D12 detects CTD Tyr[1] phosphorylation in HeLa cells (Input). Pol II was immunoprecipitated with antibody 1C7 (IP 1C7, fig. S1) and incubated with cAbl kinase, leading to a 3D12 signal (IP+cAbl). The hyper- (IIO) and hypophosphorylated forms (IIA) of Pol II are indicated.

[1]Gene Center and Department of Biochemistry, Center for Integrated Protein Science Munich (CIPSM), Ludwig-Maximilians-Universität München, Feodor-Lynen-Strasse 25, 81377 Munich, Germany. [2]Department of Molecular Epigenetics, Helmholtz Zentrum München and CIPSM, Marchioninistrasse 25, 81377 Munich, Germany. [3]Institute of Molecular Immunology, Helmholtz Zentrum München, Marchioninistrasse 25, 81377 Munich, Germany.

*These authors contributed equally to this work.
†To whom correspondence should be addressed. E-mail: eick@helmholtz-muenchen.de (D.E.); cramer@genzentrum.LMU.de (P.C.).

Ser[2], and Ser[5]. A correlation between levels of Tyr[1] phosphorylation and mRNA expression (*15*) (fig. S5A) further indicated that Tyr[1] phosphorylation is functionally relevant.

Gene-averaging of ChIP profiles (*14*) revealed Tyr[1] phosphorylation in the coding region (Fig. 2, A and B). Whereas Tyr[1] phosphorylation signals were low at promoters, they increased downstream of the transcription start site (TSS). The gene-averaged profile resembled that for Ser[2] phosphorylation, except that Ser[2] phosphorylation signals persist downstream of the polyadenylation (pA) site for ~200 nucleotides (nt), whereas Tyr[1] phosphorylation signals decrease already around 180 nt upstream of the pA site (Fig. 2, A, B, and D). The point of Tyr[1] phosphorylation signal increase was dependent on the TSS, whereas the point of decrease was dependent on the pA site but not on gene length or expression level (Fig. 2D and figs. S5B and S6). These results indicate that Tyr[1] phosphorylation marks are set and removed within the transcription cycle.

To investigate whether Tyr[1] phosphorylation influences factor recruitment to Pol II, we determined genomic occupancy profiles for termination factors Nrd1, Rtt103, and Pcf11, which contain a CTD-interacting domain (CID). The gene-averaged Nrd1 occupancy peaked at the beginning of the transcribed region, 193 ± 44 nt downstream of the TSS (Fig. 2C). This region also showed maximum signals in Ser[5] phosphorylation, and genomic Nrd1 and Ser[5] phosphorylation profiles correlate (R = 0.6), consistent with Nrd1 binding to the Ser[5]-phosphorylated CTD (*16*). The general presence of Nrd1 at protein-coding genes extends previous results (*17*, *18*) and befits a role of Nrd1 in early transcription termination (*2*, *19*–*21*). Rtt103 showed peak occupancy at the end of genes, 112 ± 27 nt downstream of the pA site, where peak levels of Pcf11 were also observed (*14*) (Fig. 2C and fig. S7). Because this region shows the maximum difference between Ser[2] and Tyr[1] phosphorylation signals, Tyr[1] phosphorylation may impair recruitment of Rtt103 and Pcf11 upstream of the pA site. Consistent with this, genome-wide occupancies of Rtt103 and Pcf11 do not correlate well with Ser[2] phosphorylation signals (R = 0.4, for both), although both proteins bind the Ser[2]-phosphorylated CTD (*22*, *23*).

To test whether Tyr[1] phosphorylation impairs CTD binding of termination factors, we determined the affinity of purified recombinant CIDs of yeast Nrd1, Pcf11, and Rtt103 for various CTD diheptad phosphopeptides (table S1) by using fluorescence anisotropy (Fig. 3, A to C, and fig. S8). None of the CIDs bound to an unphosphorylated CTD peptide. Consistent with previous results (*16*, *23*), Pcf11-CID and Rtt103-CID bound to the Ser[2]-phosphorylated CTD peptide [dissociation constants (K_D) = 54 ± 6 μM (±SD) and 12 ± 2 μM, respectively; Methods], whereas the Nrd1-CID preferentially bound to a Ser[5]-phosphorylated CTD peptide (K_D = 85 ± 25 μM). In contrast, none of the CIDs bound Tyr[1]-phosphorylated CTD peptides, regardless of whether additional phosphorylations were present or not. Thus, Tyr[1] phosphorylation blocks CID binding to the CTD in vitro, consistent with the hypothesis that it impairs termination factor recruitment in vivo.

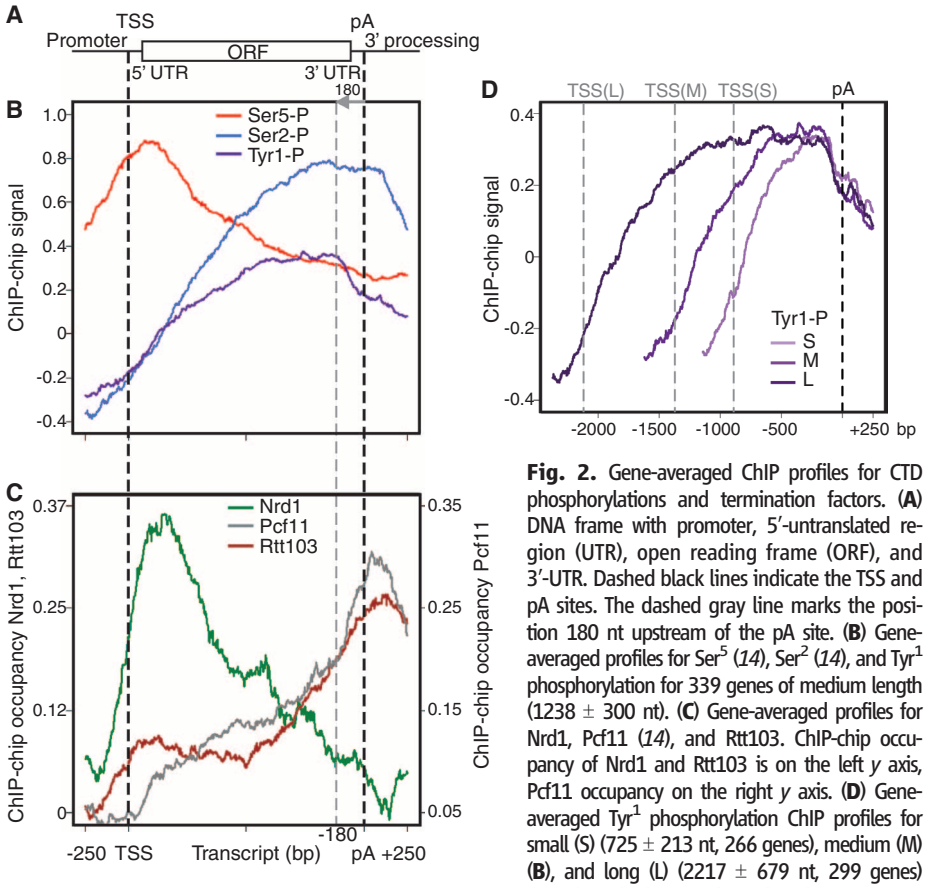

Fig. 2. Gene-averaged ChIP profiles for CTD phosphorylations and termination factors. (**A**) DNA frame with promoter, 5′-untranslated region (UTR), open reading frame (ORF), and 3′-UTR. Dashed black lines indicate the TSS and pA sites. The dashed gray line marks the position 180 nt upstream of the pA site. (**B**) Gene-averaged profiles for Ser[5] (*14*), Ser[2] (*14*), and Tyr[1] phosphorylation for 339 genes of medium length (1238 ± 300 nt). (**C**) Gene-averaged profiles for Nrd1, Pcf11 (*14*), and Rtt103. ChIP-chip occupancy of Nrd1 and Rtt103 is on the left *y* axis, Pcf11 occupancy on the right *y* axis. (**D**) Gene-averaged Tyr[1] phosphorylation ChIP profiles for small (S) (725 ± 213 nt, 266 genes), medium (M) (**B**), and long (L) (2217 ± 679 nt, 299 genes) gene-length classes, aligned at the pA site.

Structural modeling reveals how Tyr[1] phosphorylation blocks the CID-CTD interaction. Crystal structures of Ser[2]-phosphorylated CTD peptides bound to Pcf11-CID (*22*) and Rtt103-CID (*23*) are available, and the structure of the Nrd1-CID (*16*) is known. In the Pcf11-CTD structure, the Tyr[1] hydroxyl group forms a hydrogen bond with the Asp[68] side chain in the CID (*22*) (fig. S9A). This indicates that Tyr[1] phosphorylation blocks CTD binding because of electrostatic repulsion of two negatively charged groups, the Asp[68] side chain and the Tyr[1] phosphate. The CTD-binding aspartate residue is conserved in the Nrd1 CID (*16*). In the Rtt103-CTD structure, the corresponding residue, Asn[65], forms a hydrogen bond with the Tyr[1] hydroxyl group (*23*) that is incompatible with Tyr[1] phosphorylation. Generally, a Tyr[1] phosphate group modeled onto CTD peptides in CID complex structures results in steric clashes (fig. S9B).

Structural considerations also indicated that Thr[4] phosphorylation (*10*) interferes with CID binding by destabilizing the bound CTD conformation (*22*). This predicted that Thr[4] phosphorylation levels at the pA site are low, to enable recruitment of Pcf11 and Rtt103. Indeed, ChIP profiling revealed that Thr[4] phosphorylation is limited to the transcribed region (fig. S10). Modeling further indicated that Ser[7] phosphorylation is unlikely to interfere with CTD-CID binding, consistent with Nrd1 recruitment in the 5′ region of genes where Ser[7] phosphorylation levels are high (*14*). Thus, genome-wide signals of CTD phosphorylation at Thr[4] and Ser[7] are consistent with the function of Tyr[1] phosphorylation in impairing termination factor recruitment.

To investigate whether Tyr[1] phosphorylation also impairs CTD interactions of factors with other CTD-binding domains, we investigated the tandem Src homology 2 (SH2) domain of elongation factor Spt6. This domain binds the Ser[2]-phosphorylated CTD (*24*–*27*) and is required for high Spt6 occupancy on transcribed genes (*14*), suggesting that Tyr[1] phosphorylation does not interfere with its CTD binding. Indeed, the recombinant domain (residues 1250 to 1444) bound very well to CTD peptides phosphorylated at Tyr[1], Tyr[1] and Ser[2], or Tyr[1] and Ser[5] but not to unphosphorylated CTD (Fig. 3D). These results were consistent with recent data (*26*, *27*) and showed that interactions with Tyr[1]-phosphorylated CTD peptides were even stronger than for peptides with phosphorylations at Ser[2] or Ser[5] alone. This shows that Tyr[1] phosphorylation stimulates CTD binding of a bona fide elongation factor.

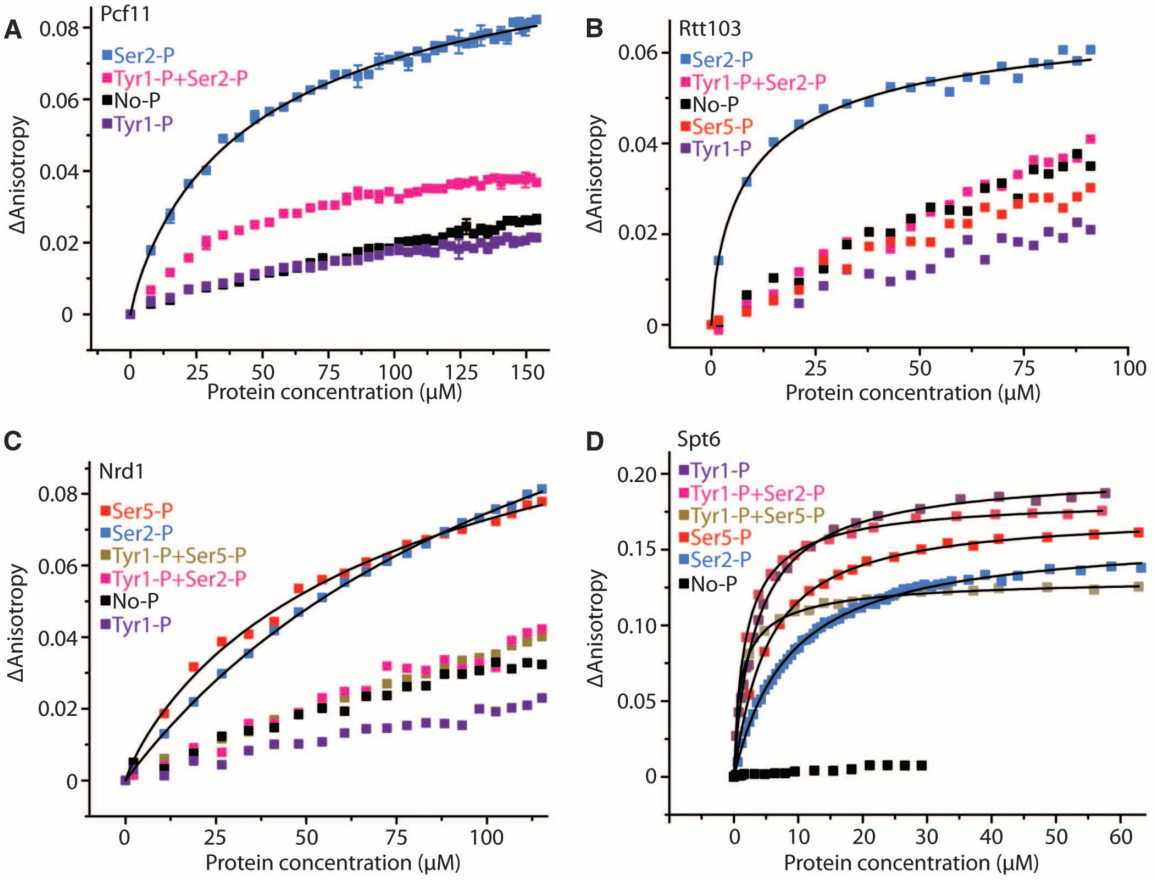

Fig. 3. CTD Tyr[1] phosphorylation blocks termination factor binding. Fluorescence anisotropy titration of CTD peptides with recombinant Pcf11-CID (**A**), Rtt103-CID (**B**), Nrd1-CID (**C**), and Spt6 tandem SH2 domain (**D**). When possible, binding affinity was determined as the protein concentration at half-maximum binding by nonlinear Hill fit (Origin). The remaining affinity of Pcf11-CID for the Tyr[1]/Ser[2]-phosphorylated CTD peptide was not observed at higher salt concentration (fig. S7). Tyr[1]-phosphorylated CTD peptides were not bound by CIDs [(A) to (C)], but by Spt6 tandem SH2 domain (for Tyr1-P, K_D = 3.6 ± 0.15 μM; Tyr1-P+Ser2-P, K_D = 1.9 ± 0.04 μM; Tyr1-P+Ser5-P, K_D = 1.3 ± 0.06 μM; Ser2-P, K_D = 8.4 ± 0.19 μM; Ser5-P, K_D = 5.2 ± 0.09 μM).

We tested whether Tyr[1] phosphorylation depends on one of the yeast CTD kinases, Kin28, Srb10, Bur1, or Ctk1, which correspond to human Cdk7, Cdk8, Cdk9, and Cdk12, respectively. Inhibition of these kinases in vivo did not significantly affect Tyr[1] phosphorylation signals (table S2 and fig. S11). This indicates that Tyr[1] phosphorylation of the yeast CTD depends on a kinase other than the known CTD kinases. Consistent with this, Tyr[1] phosphorylation in human cells is achieved by c-Abl (*13*), a kinase that lacks a yeast homolog.

Our results extend the previously proposed CTD code (*3*, *28*, *29*), which was based on Ser[2] and Ser[5] phosphorylation, leading to an extended CTD code for the coordination of the transcription cycle with factor recruitment (fig. S12). During initiation and early elongation, the CTD is phosphorylated on Ser[5], which facilitates recruitment of the capping enzyme and Nrd1. Peak occupancy levels are reached for Nrd1 and Pol II 150 to 200 nt downstream of the TSS (*14*), likely marking a decision point where Pol II transiently pauses and either terminates or continues elongation (*2*). When Tyr[1] and Ser[2] phosphorylation levels rise, Pol II binds elongation factors stably and continues elongation. Tyr[1] phosphorylation releases Nrd1 and impairs recruitment of Rtt103 and Pcf11, suppressing termination during elongation. Before the pA site, Tyr[1] phosphorylation levels drop, whereas Ser[2] phosphorylation levels remain high. This enables recruitment of Rtt103 and Pcf11 that is enhanced by cooperative interactions between factors (*23*) and with nascent RNA (*18*), resulting in 3′-RNA processing and transcription termination. Our results indicate that Tyr[1] CTD phosphorylation is a target to activate transcription by suppressing Pol II termination and explain why mutation of Tyr[1] to phenylalanine, which lacks the oxygen atom required for phosphorylation, is lethal (*30*).

References and Notes

1. R. D. Chapman, M. Heidemann, C. Hintermair, D. Eick, *Trends Genet.* **24**, 289 (2008).
2. S. Buratowski, *Mol. Cell* **36**, 541 (2009).
3. J. L. Corden, *Science* **318**, 1735 (2007).
4. P. Komarnitsky, E.-J. Cho, S. Buratowski, *Genes Dev.* **14**, 2452 (2000).
5. S. C. Schroeder, B. Schwer, S. Shuman, D. Bentley, *Genes Dev.* **14**, 2435 (2000).
6. S. H. Ahn, M. Kim, S. Buratowski, *Mol. Cell* **13**, 67 (2004).
7. R. D. Chapman *et al.*, *Science* **318**, 1780 (2007).
8. M. Kim, H. Suh, E.-J. Cho, S. Buratowski, *J. Biol. Chem.* **284**, 26421 (2009).
9. S. Egloff *et al.*, *Science* **318**, 1777 (2007).
10. J.-P. Hsin, A. Sheth, J. L. Manley, *Science* **334**, 683 (2011).
11. R. Baskaran, M. E. Dahmus, J. Y. Wang, *Proc. Natl. Acad. Sci. U.S.A.* **90**, 11167 (1993).
12. J. W. Stiller, M. S. Cook, *Eukaryot. Cell* **3**, 735 (2004).
13. R. Baskaran, S. R. Escobar, J. Y. J. Wang, *Cell Growth Differ.* **10**, 387 (1999).
14. A. Mayer *et al.*, *Nat. Struct. Mol. Biol.* **17**, 1272 (2010).
15. S. Dengl, A. Mayer, M. Sun, P. Cramer, *J. Mol. Biol.* **389**, 211 (2009).
16. L. Vasiljeva, M. Kim, H. Mutschler, S. Buratowski, A. Meinhart, *Nat. Struct. Mol. Biol.* **15**, 795 (2008).
17. H. Kim *et al.*, *Nat. Struct. Mol. Biol.* **17**, 1279 (2010).
18. T. J. Creamer *et al.*, *PLoS Genet.* **7**, e1002329 (2011).
19. K.-Y. Kim, D. E. Levin, *Cell* **144**, 745 (2011).
20. E. J. Steinmetz, N. K. Conrad, D. A. Brow, J. L. Corden, *Nature* **413**, 327 (2001).
21. A. G. Rondón, H. E. Mischo, J. Kawauchi, N. J. Proudfoot, *Mol. Cell* **36**, 88 (2009).
22. A. Meinhart, P. Cramer, *Nature* **430**, 223 (2004).
23. B. M. Lunde *et al.*, *Nat. Struct. Mol. Biol.* **17**, 1195 (2010).
24. M. Sun, L. Larivière, S. Dengl, A. Mayer, P. Cramer, *J. Biol. Chem.* **285**, 41597 (2010).
25. M.-L. Diebold *et al.*, *J. Biol. Chem.* **285**, 38389 (2010).
26. D. Close *et al.*, *J. Mol. Biol.* **408**, 697 (2011).
27. J. Liu *et al.*, *J. Biol. Chem.* **286**, 29218 (2011).
28. S. Buratowski, *Nat. Struct. Mol. Biol.* **10**, 679 (2003).
29. S. Egloff, S. Murphy, *Trends Genet.* **24**, 280 (2008).
30. M. L. West, J. L. Corden, *Genetics* **140**, 1223 (1995).

Acknowledgments: We thank S. Etzold and K. Leike for help and S. Hahn for providing yeast strains. P.C. was supported by the Deutsche Forschungsgemeinschaft (DFG), SFB646, SFB960, TR5, NIM, the BioImaging Network, a European Research Council (ERC) Advanced Grant, and the Jung-Stiftung. D.E. was supported by DFG, TR5, and SFB684. Microrray data have been deposited in ArrayExpress under accession code E-MTAB-1060. A.M. carried out ChIP-chip and fluorescence anisotropy experiments. M.H. and C.H. validated antibodies. M.L. analyzed ChIP-chip data. M.S. carried out modeling. A.S. carried out additional ChIP assays. E.K. generated the 3D12 antibody. D.E. and P.C. designed and supervised research. A.M. and P.C. prepared the manuscript, with help from all authors.

Supplementary Materials

www.sciencemag.org/cgi/content/full/336/6089/1723/DC1
Materials and Methods
Figs. S1 to S12
Tables S1 and S2
References (*31*–*35*)

25 January 2012; accepted 7 May 2012
10.1126/science.1219651